COMMISSION A: Electromagnetic Metrology
(November 2013 – October 2016)

Edited by

Mitsuru Musha (University of Electro-communications) and

Masatoshi Kajita (National Institute of Information and Communications Technology)

A1. Time and Frequency Standards and Time Transfer Technique

The researches and developments on time and frequency standards and time transfer in Japan are mainly carried out in National Metrology Institute of Japan (NMIJ) and National Institute of Information Technology (NICT)

In NMIJ, the second cesium fountain, NMIJ-F2, for primary frequency standards has been developed. The frequency stability reaches $8.3\times10^{-14}\tau^{-1/2}$ (τ: averaging time) using an ultra-stable local oscillator and high atom number [Takamizawa et al., 2014]. The local oscillator is a cryogenic sapphire oscillator using an ultra-low-vibration pulse-tube cryocooler and cryostat. The high atom number is achieved by high power of the cooling laser beams and optical pumping to the Zeeman sublevel $m_F = 0$. In addition, the type B uncertainty has been evaluated to be 7×10^{-16} without the inclusion of uncertainty by the minor effects [Takamizawa et al., 2015a]. Moreover, NMIJ-F2 was used for absolute frequency measurement of our Sr optical lattice clock as a transfer oscillator [Tanabe et al., 2015]. Besides, external cavity diode lasers with low frequency drift have been developed for long-term operation of the fountain [Takamizawa et al., 2015b, Takamizawa et al., 2016].

Ultrastable microwave oscillators: Two liquid-helium-cooled cryogenic sapphire-resonator oscillators (CSOs), have been modified to operate using cryo-refrigerators and low-vibration cryostats [Ikegami et al., 2016]. The Allan deviation of the first cryo-refrigerator-cooled CSO (cryoCSO) was evaluated to be better than 2×10^{-15} for averaging times of 1 s to 30 000 s, which is better than that of the original liquid helium cooled CSO. It is now used with our Cs atomic fountain frequency standard, NMIJ-F2, which has achieved nearly quantum-projection-noise-limited frequency stability. The Allan deviation of the second cryoCSO is better than 4×10^{-15} from 1 s to 6 000 s averaging time.

At present four active hydrogen maser frequency standards and three cesium atomic clocks with high-performance beam tubes (Agilent 5071A) are operated at NMIJ for time keeping. Those atomic clocks are kept in individual chambers, whose temperatures are kept to within 0.2 deg C. One of the hydrogen masers is used as a source oscillator for the generation of UTC (NMIJ) to improve the short-term stability. UTC (NMIJ) is created by frequency-steering the hydrogen maser output signal to UTC using a frequency stepper.

In NMIJ, Dual frequency carrier phase GPS receiver is one of the main international time and frequency transfer tools. NMIJ has the Two Way Satellite Time and Frequency Transfer (TWSTFT) facilities for Asia Pacific link and for Asia-European link.

Frequency Calibration Service at NMIJ; NMIJ has been providing the remote frequency calibration service using the GPS common-view method and Internet since 2006. The CMCs of the service are 1.1×10^{-13} (baseline: 50 km), 1.4×10^{-13} (baseline: 500 km) and 4.9×10^{-13} (baseline: 1,600 km) at an averaging time of one day. The number of users is 20 in 2016; it is on the rise year by year.

NICT and TL have evaluated a software-defined receiver (SDR) comprising a high-resolution correlator and successive interference cancellation associated with open-loop configuration in order to improve the stability of operational two-way satellite time and frequency transfer (TWSTFT) [Huang et al, 2016]. According to the result of the measurements TWSTFT receiver reduces the time deviation from 140 ps to 73 ps at averaging time of 1 h, and occasionally suppresses diurnals. NICT developed a state-of-art system for the remote frequency comparison of optical clocks without a flywheel oscillator at the remote end. The system uncertainty and instability to be at the low 10^{-15} level using an Sr lattice clock [Fujieda et al., 2016].

Fundamental research of chip scale atomic clock (CSAC) has been performed in Tokyo Metropolitan University (TMU) and NICT. In TMU, Ramsey spectrum was observed using pulsed laser, with which high frequency stability is obtained with lower electric power [Yano et al., 2014] [Yano et al., 2015]. In NICT, development of chip scale atomic clock (CSAC) started. The possibility to improve the frequency stability by using the phase modulation is being searched.

Broadband VLBI system GALA-V has been developed by NICT [Sekido et al., 2016]. The GALA-V is aimed to make long distance frequency comparison between small diameter antennas via broadband VLBI observation. A series of test experiments between NICT and NMIJ have been conducted in 2016. About one pico second delay precision group delay measurement has been achieved with small diameter antenna pair. It is getting clear that total observation error is dominated by atmospheric uncertainty [Kondo et al., 2016].

A2. Laser Stabilization & Frequency Measurement

The researches and developments on laser stabilization and frequency measurement in Japan, especially, the accuracy improvement of ^{87}Sr lattice clock ($^1S_0$-$^3P_0$ transition), are mainly carried out NICT, NMIJ and RIKEN - University of Tokyo group.

At NICT, the uncertainty of the absolute frequency of ^{87}Sr lattice clock has been reduced to 9.3×10^{-16} and its systematic uncertainty has been deuced down to 8.6×10^{-17}. The direct comparison with Sr lattice clock in Physicarische Technische Bundesanstalt (PTB, Germany) has been performed, and the difference was measured to be (1.1±1,6) x 10^{-15} [Hachisu, 2014]

[Hachisu, 2015]. In NICT, a new method to use the Sr lattice clock to calibrate UTC-NICT was developed. Measurement of three hours every one or two weeks was continued for five months, and the discrepancy from the SI time scale was maintained to be less than 2 ns [Ido, 2016] .

At NMIJ, the uncertainty of the absolute frequency of the ^{87}Sr lattice clock ($^1S_0$-$^3P_0$ transition) has been measured to be 3.7 x 10^{-15} in 2014 [Akamatsu, 2014]. The uncertainty of the absolute frequency measurement was mainly limited by that of the comparison with the NMIJ coordinated universal time (UTC(NMIJ)). To reduce the uncertainty, a Cs atomic fountain clock was used as a local oscillator to monitor the frequency variation of UTC(NMIJ) during the measurements in 2015 [Tanabe, 2015]. Consequently, the uncertainty was reduced to 1.2 x 10^{-15}. The frequency ratio of the clock transitions in Sr and Yb was measured by an optical direct frequency link between two independent optical lattice clocks of Sr and Yb in 2014. The fractional uncertainty of the measurement was 1.4 x 10^{-15} [Akamatsu, 2014a] [Akamatsu, 2014b]. A dual optical lattice clock has been being developing at NMIJ since 2009.

Katori group at the University of Tokyo and RIKEN has been developing optical lattice clocks with strontium (Sr), ytterbium (Yb) and mercury (Hg) atoms. They have also developed an optical frequency transfer system using a fiber link between the two sites to demonstrate remote frequency comparison at the level of 10^{-18} uncertainties.

In 2015, RIKEN group developed two cryogenic Sr optical lattice clocks. Thus far, the accuracy of Sr optical lattice clocks has been limited by the uncertainty of ambient blackbody radiation shift. By installing a cryogenic chamber, they have succeeded in reducing the uncertainties of blackbody radiation shifts to $9x10^{-19}$ and compared two cryogenic Sr lattice clocks with the uncertainties of $5x10^{-18}$ [Ushijima et al., 2015]. RIKEN group has also developed optical lattice clocks with Hg atoms. Hg atoms have one order of magnitude smaller sensitivity to the blackbody radiation than Sr and Yb atoms. This allows realizing the uncertainties of 10^{-18} even in a room-temperature environment. They compared the frequencies between Hg and Sr optical lattice clocks using a phase-stabilized optical frequency comb and determined the frequency ratio with the uncertainties of $8.4x10^{-17}$ [Yamanaka et al., 2015].

As a physical property of Yb atoms is similar to that of Sr, Sr optical lattice clocks can share the setup with Yb clocks. RIKEN group has modified one of the cryogenic Sr optical lattice clocks to be compatible with Yb optical lattice clocks. They have performed frequency comparison between Sr and Yb optical lattice clocks and determined the frequency ratio with $4.6x10^{-17}$ uncertainties, which is the best accuracy obtained so far between two different atomic species [Nemitz et al., 2016].

Frequency comparison between two remote Sr optical lattice clocks operated in the University of Tokyo and RIKEN was performed via a phase-stabilized optical fiber link with their direct distance of 15 km. The frequency comparison of the remote clocks measures the relative frequency difference to be 1,653.3(7.5)x10^{-18}, which corresponds to the gravitational red shift due to the height difference of 1,516(5) cm. The result agrees well with the altitude difference measured by conventional spirit leveling performed by Geospatial Information Authority of Japan. The centimeter-level remote clocks' comparison will become a building block of future clock network for relativistic geodesy and fundamental science [Takano et al., 2016].

In NICT, a new frequency standard based on the In^+ $^1S_0$-$^3P_0$ transition frequency is under development, and the result was close to the measurement obtained by the Erlangen group. The uncertainty of the order of 10^{-15} is going to be attained.

The attainable accuracies of vibrational transition frequencies of homonuclear diatomic molecular ions were theoretically estimated [Kajita et al., 2014]. For the pure vibrational transition frequencies of N_2^+ (with zero nuclear) [Kajita, 2015].

The apparatus for the precise measurement of THz-wave has been developed in NICT [Nagano et al., 2013] [Ito et.al., 2013].

Hong group at Yokohama National University is developing optical frequency combs and frequency stabilized lasers. They have developed a compact iodine-stabilized laser with stability at the 10^{-12} level using a coin-sized laser module [Kobayashi et al. 2015]. This laser has been recommended by the International Committee for Weights and Measures (CIPM) as an optical frequency standard at 531 nm. The compact laser has been applied to long gauge block measurements [Bitou, 2016].

Sugiyama group at Kyoto University has been developing Yb^+ and Ba+ ion clocks. The group aims at search for a temporal variation of the fine-structure constant. They succeeded in single-ion spectroscopy of the $^2S_{1/2}$—$^2D_{3/2}$ transition at 435 nm in ^{171}Yb with a spectral width of 380 Hz [Imai et al., 2016]. They observed resolved motional sidebands in the spectra of the $^2S_{1/2}$—$^2D_{5/2}$ transition at 1.76 μm in single $^{138}Ba^+$. They succeeded in laser cooling of single $^{137}Ba^+$ ions which have a clock transition of a low sensitivity to electric quadrupole field [Fujisaki et al., 2016]. They are developing optical frequency-ratio measurement system using octave-spanning optical frequency combs based on mode-locked titanium-doped sapphire lasers and ytterbium-doped potassium-yttrium-tungstate (Yb:KYW) lasers [Mitaki et al., 2014].

Nakagawa group at University of Electro-communications (UEC) has developed an optical frequency synthesizer for the precision spectroscopy of highly excited Rydberg states of Rb atoms. This synthesizer can generate widely tunable 480 nm laser light with an optical power of 150 mW and an absolute frequency uncertainty of less than 100 kHz using a high repetition rate (325 MHz) Er fiber-based optical frequency comb and a tunable frequency-doubled diode laser at 960 nm. We demonstrate the precision two-photon spectroscopy of Rydberg states of ^{87}Rb atoms by observing electromagnetically induced transparency on a vapor cell, and measure the absolute transition frequencies of ^{87}Rb to *nD* and *nS* Rydberg states with an uncertainty of less than 130 kHz [Watanabe, 2016]. The measured transition frequencies of Rydberg excitation of Rb are useful for the recent applications in quantum information processing, quantum simulations using Rydberg atoms.

Musha group at UEC has developed the optical frequency comb which is based on Er-doped fiber mode-lock laser for wideband frequency reference and dual comb spectroscopy, the precision remote dissemination of the reference signal through the long optical fibers and space-borne frequency stabilized lasers. For the Japanese space gravitational wave detector named DECIGO, we have developed the stable and high-power Yb-doped fiber lasers whose frequency is stabilized in reference to the saturated absorption of iodine at 515 nm to obtain short- and long term frequency stability, and the intensity noise is also stabilized to $dI/I = 2\text{x}10^{-8}$ /√Hz at the observation band of DECIGO around 1 Hz. The compact and robust two breadboard models are now under development for the future space borne stable lasers [Suemasa, 2016].

A3. Realization of Electrical Unit (DC & LF)

Research works and developments on dc and low frequency electrical standards are implemented in the electrical standards area of Research Institute for Physical Measurement in NMIJ, partly in collaboration with several other institutes in the Advanced Industrial Science and Technology (AIST). In the five research groups of the electrical standards area, the Applied Electrical Standards Group and the Quantum Electrical Standards Group covers A3 Field.

The Quantum Electrical Standards group has developed an integrated quantum voltage noise source (IQVNS) that is fully implemented with superconducting circuit technology for Johnson noise thermometry (JNT) [Urano et al, 2016]. For precise measurements of Boltzmann's constant, the IQVNS chip was designed to produce intrinsically calculable pseudo-white noise to calibrate JNT systems. On-chip real-time generation of pseudo random codes with simple circuits achieved pseudo voltage noise with a harmonic tone interval less than 1 Hz, which was one order of magnitude finer than those of conventional quantum voltage noise sources.

A liquid-helium-free PJVS has been utilized since 2015 for calibrations of Zener voltage standards with the CMC values, 8.0 nV for 1 V and 45 nV for 10 V, same as those for our conventional JVS system cooled with liquid helium [Takahashi et al., 2015]. The first direct comparison between our cryocooler-based PJVS system and the BIPM's new transportable PJVS system that is cooled with liquid helium has been carried out at NMIJ. The agreement within 5×10^{-12} at the output DC level of 10 V was confirmed between both the systems [Chen et al., 2015]. We are now attempting to develop an AC voltage calibration system using PJVS [Maruyama et al., 2015a]. Development of Zener voltage standards are also now in progress in collaboration with ADC Corporation [Maruyama et al., 2015b].

Fig.1 Prototype of a Zener votage standard.

Development of compact and ultra-stable 1 Ω, 10 Ω, 100 Ω and 1 kΩ standard resistors has been finished [Kaneko et al., 2016a] [Domae et al., 2015a], and 10 kΩ resistors are in progress of evaluation and development. In 2016, we have finalized ~4 years of evaluation of 1 Ω and 10 Ω resistors, and the drift rates of those range of resistors are around 0.05 ppm/year and the temperature coefficients are around less than 0.1 ppm/˚C. Vibration test has been also carried out for 100 Ω resistors and showed no effect by the harsh (frequency: 16.7 Hz, amplitude: 4 mm in 3 axes) condition. It is demonstrated that this excellent performance is suitable for utilization in national metrology institutes and international comparisons

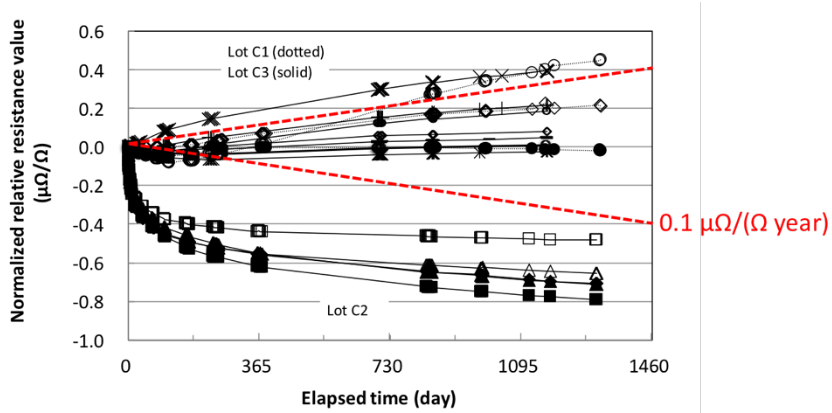

Fig. 2 Resistance histories (drifts) of 1Ω resistors.

Conventional single Hall bar QHR devices have been fabricated and several devices have been provided for several NMIs [Domae et al., 2015b].

Newly designed 1 MΩ quantum Hall array resistance standard devices also have been fabricated. This device consists of 88 Hall bars on 8 × 8 mm^2 GaAs/AlGaAs chip and its nominal value has only -0.0342 ppm difference based on R_{K-90} from the integer value of 10^6.

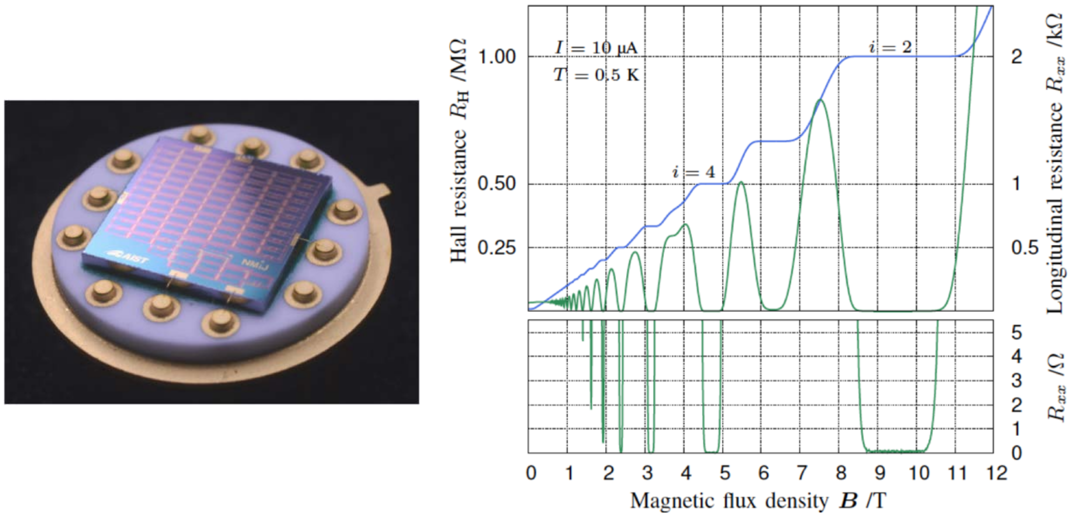

Fig. 3 Picture and Hall and longitudinal resistance curve of 1 MΩ array device.

To establish a relationship between the physical structure of electrical contact boundary and contact resistance, NMIJ developed a method for evaluating that using a physical simulated sample created via nanofabrication. Several samples with various diameter of "contact area" were made and their resistances were measured precisely. After removing influence of thickness of electrodes, it was demonstrated experimentally that our result is in good agreement with an expression for constriction resistance.

Towards a realization of the current standard based on the single-electron pumping, we investigate the physics of low-temperature electron transport phenomena in various types of single-electron devices, i.e. superconductor-insulator-normal-insulator-superconductor (SINIS) turnstiles, gate-confined quantum dots, and graphene- or nanotube-based single-electron transistors [Kaneko et al., 2016b].

On SINIS turnstiles, in our early studies, we had discovered the new phenomenon that is a reduction of the single-electron pumping error induced by a weak magnetic field applied to the device. However, the origin of this phenomenon had remained poorly understood. To elucidate the underlying mechanism, we performed detailed measurement and analysis. First, in order to confirm the reproducibility of this phenomenon, we compare two SINIS devices of the identical structure each of which is fabricated with the aid of completely different nano-fabrication facilities and confirm the reproducibility as well as the universality. We then elucidate the mechanism based on a numerical simulation of the quasi-particle state in the lead electrodes.

Aiming at further reducing the pumping error, we extended the research to that based on another pumping mechanism. In one instance, we investigated a GaAs-based gate-defined quantum dot and demonstrated single-parameter pumping. In addition, we developed an air-bridge based parallel integration of this pump to demonstrate a synchronized parallel pumping that can generate a larger current otherwise unattained [Nakamura et al., 2015]. In this study, molecular beam epitaxy growth of high-quality and gate-stable GaAs hetero-structure wafer is critical for the further development of the pumping accuracy. So, the improvement of the wafer quality is our future plan.

In addition to the single electron pumping, we start the experiment of the error counting using RF-reflectometry. The ac signal around a few hundred MHz signal is applied to the matching circuits in the dilution refrigerator. Using homodyne detection, we can succeed to detect the few tens MHz of impedance change of the device. Also we fabricated the capacitive coupled single electron device, namely single electron pumping device and single electron counter. Now we have plan auto correction system using arbitrary wave generator, FPGA and charge detector. This will make the improvement of the pumping accuracy and give us the intuitive information of the origin of charge pump errors. Alongside of these experiments, we also developed a new dilution refrigerator setup for measuring tiny ac current by employing low-noise superconducting-quantum-interference-device-based current amplifier as the first-stage amplifier. The measured current noise floor of this setup was at least one order of magnitude improved than that obtained with the setup that employs a semiconductor-based cryogenic current amplifier at the first-stage. We plan to take advantage of this setup to investigate various kinds of phenomena including non-equilibrium electron transport in mesoscopic devices and micro electromechanical systems.

These single-electron devices are planned to be integrated with the quantum metrology triangle experiment that combine the single-electron device with the quantum Hall resistance and Josephson voltage standards. Towards this futuristic experiment, we had introduced a dry dilution refrigerator; the large sample open space offered by this refrigerator allows us to integrate the whole components required for the triangle experiment including a cryogenic current comparator into one system. Electric noise filters and high-frequency wiring are now designed and constructed to complete this setup.

We have been studying for measuring electric characteristics of lithium-ion batteries (LIBs) and super-capacitors by using an impedance spectroscopy method. Aim of this work is to establish the precision testing technique of charge-discharge cycle dependence of the characteristics which can provide an effective tool to examine the lifetime prediction of the energy-storage devices. Cycle dependence of impedance was measured for cylindrical 18650-type LIBs by our electrochemical impedance measurement system. We obtained the relation of charge-discharge cycle vs internal resistance components which were estimated based on the results of the impedance and on the equivalent circuit models. We are now engaging the improvement of the measurement system including measurement fixtures which are suitable for lamination-type batteries.

NMIJ has started a calibration service for rechargeable battery's impedance meters. Calibration range, 1 Ω - 100 Ω at 1 kHz, is a crucial for monitoring the long-term performance behavior of the batteries under test. Expanded uncertainties were estimated to be 0.13 mΩ/Ω in the range from 1 Ω to 10 Ω and to be 25 μΩ/Ω in the range from 10 Ω to 100 Ω (*k* = 2).

Fig. 4 Electrochemical impedance measurement system and fixture for measuring 18650-type batteries.

AC resistor calibration service has been kept in the range of 10 Ω up to 100 kΩ at 1 kHz and 10 kHz. Standard capacitor (dry-nitrogen or used silica dielectric) calibration service has been kept in the range of 10 pF up to 1000 pF at 1 kHz, 1.592 kHz.

NMIJ has provided ac-dc voltage difference transfer calibration of thermal converters in the voltage range from 10 mV to 1000 V and in the frequency range from 10 Hz to 1 MHz. We have been participating in APMP Comparison for "APMP.EM-K12" of AC/DC current transfer difference.

Toward a low-frequency AC voltage standard down to 10 Hz, we have extended the voltage range from 3 V to 10 V root-mean squared amplitude in AC-DC difference measurements of a thermal-voltage converter using our AC-Programmable Josephson voltage standard system. The overall uncertainty was evaluated as 1.1 μV/V (k = 2) for the frequency of 62.5 Hz. The measurement uncertainty showed a significant improvement compared to the conventional method based on a theoretical approach in the frequency range below 100 Hz [Amagai et al., 2015a].

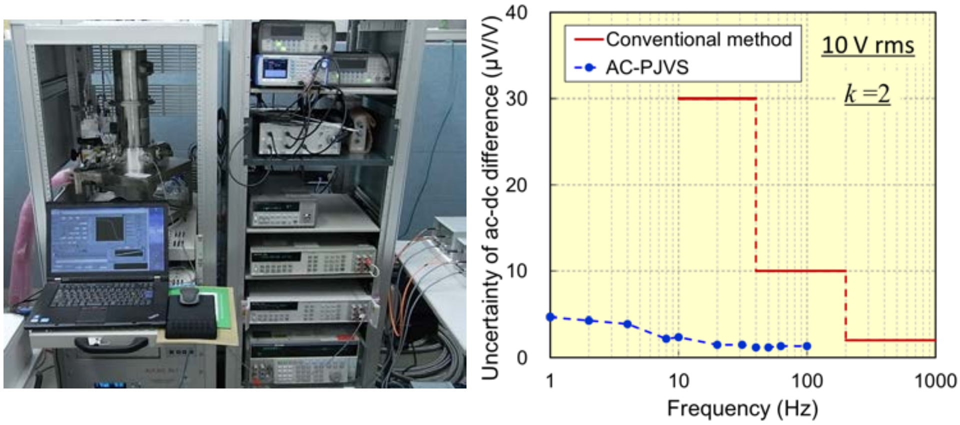

Fig. 5

With regard to a regular calibration service, we have provided a calibration service of AC voltmeters using a thermal converter in the frequency range from 4 Hz to 10 Hz, 40 Hz to 100 kHz at the RMS voltage of 10 V, and 1 V.

Toward a waste-heat recovery, we have launched a new project toward Seebeck coefficient metrology that is the most fundamental physical property in the research field of thermoelectric energy conversion. To fulfill our purpose, we have developed a new method to determine absolute Seebeck coefficient using a Thomson-coefficient integration technique, and a superconductor thermocouple technique [Amagai et al, 2015b]. So far, we have measured the absolute Seebeck coefficient of Pt using a superconductor thermocouple technique, because the thermoelectric power in the Meissner state is sufficiently small. In our experiment, by employing a $Bi_2Sr_2Ca_2Cu_3O_{10+\delta}$ superconductor, the absolute Seebeck coefficients of the Pt sample have been determined in the temperature range up to 100 K.

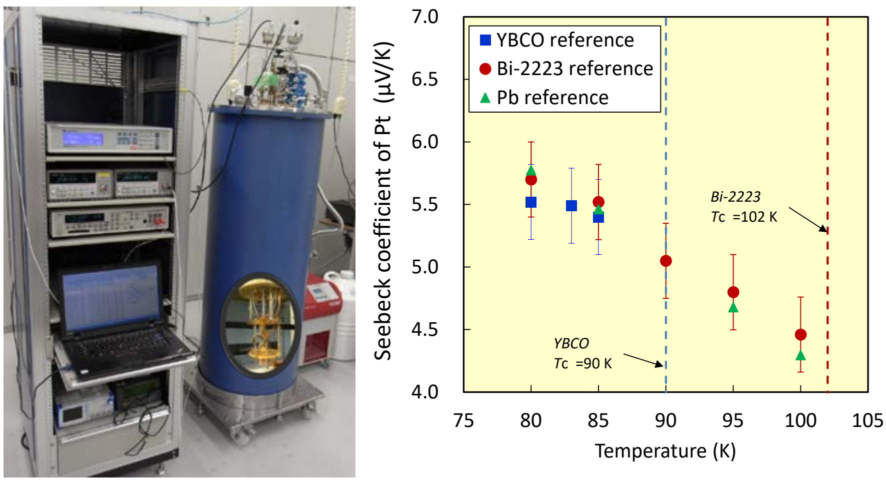

Fig. 6

A4. EM Field, Power Density and Antenna Measurement

The Electromagnetic Fields Group in the electrical standards area of NMIJ takes charge of antenna properties, electric fields and magnetic field standards.

A calibration service for the free-space antenna factor on loop antenna has been kept in the frequency range of 20 Hz to 30 MHz. The Draft A report of APMP supplementary comparison APMP.RF-S21.F is made circular among KRISS, NMIA and NMIJ since February 2017.

AC Magnetic field sensor calibration service has been kept in the range of 1 uT up to 150 uT at 50 Hz and 60 Hz.

Calibration of the dipole antenna factor above a ground plane from 30 MHz to 1 GHz with the specific conditions (with horizontal polarization and at 2.0 m from the ground surface) is available. The free space dipole antenna factor in an anechoic chamber from 1 GHz to 2 GHz is also available.

The free space antenna factor calibration service for broadband antenna for Biconical antenna (30 MHz to 300 MHz) and Log periodic dipole array antenna (300 MHz to 1000 MHz) are being performed using our original three antenna calibration method. Super broadband antenna (30 MHz to 1000 MHz) calibration service has been started from June 2015.

Calibration services for the gains of standard horn antennas are being performed from 1.7 GHz to 2.6 GHz and 18 GHz to 26.5 GHz using an extrapolation method. An antenna gain calibration service for ridged guide broadband horn antenna (1 GHz to 6 GHz) is available.

An antenna gain calibration service for millimeter-wave standard gain horn antenna is being performed form 50 GHz to 75 GHz and 75 GHz to 110 GHz using a time-domain processing and extrapolation technique.

The calibration system of monostatic Radar Cross Section (RCS) for a trihedral corner reflector in W-band has been developed. The RCS calibration range is 3 dBsm to 12 dBsm at 75 GHz and 6 dBsm to 15 dBsm at 110 GHz. This RCS range corresponds to the reflector size L ranging from 75 mm to 125 mm. The expanded uncertainty of RCS was estimated to between 0.90 dB and 1.32 dB. This RCS calibration service has been started from June 2015.

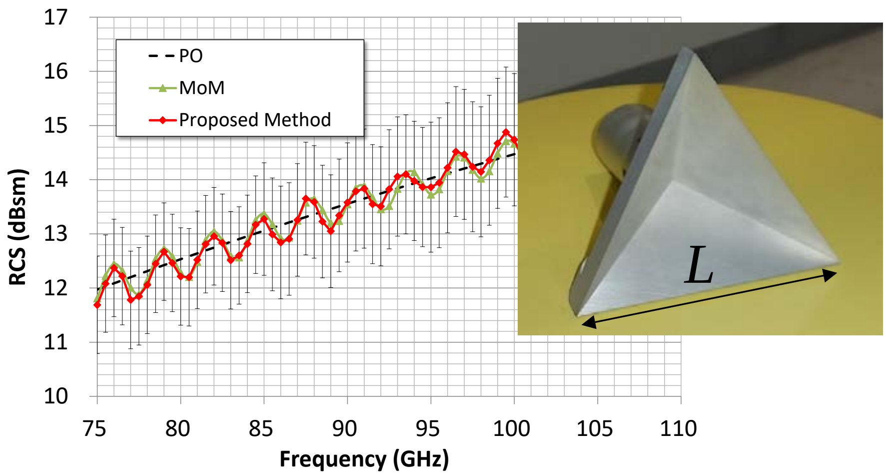

Fig. 7 RCS calibration results in W-band and an example of a trihedral corner reflector

The E-field transfer probe calibration from 20 MHz to 2 GHz in a G-TEM cell is available. The correction factor of a probe under calibration is provided when the probe output is 10 V/m. A TEM cell is employed as the standard E-field generator at low frequencies and the free space dipole antenna factor is used for the standard field generation in the anechoic chamber above 900 MHz. An optical E-field probe is employed to transfer the standard E-field strength into the G-TEM cell. [Kurikawa et al., 2016]

NMIJ has been studying a terahertz calorimeter for measuring absolute power of a terahertz beam [Shimada et al., 2015]. We have succeeded in calorimetric measurement of the absolute power at 1 THz at sub-microwatt levels. The expanded uncertainty was estimated as 2.4% at 0.59 μW. The minimum measurable power level was expanded up to 30 nW.

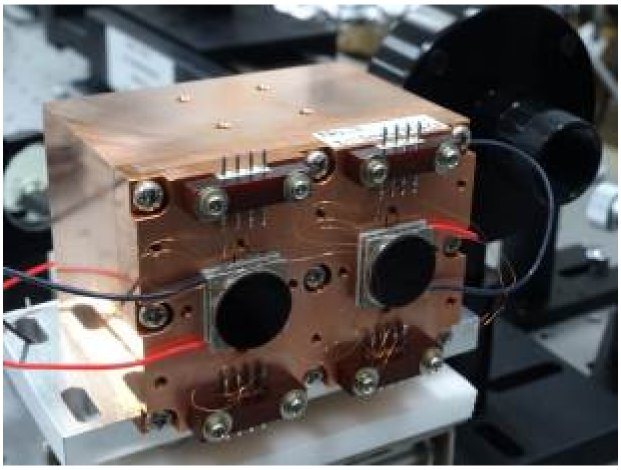

Fig. 9 Prototype of Twin type THz Caloriemeter

NMIJ has participated in a comparison of transmittance using terahertz time-domain spectrometers among three institutes (NMIJ, NICT, RIKEN) to verify equivalence of measurements from different measurement systems. We have discussed to provide practice guidelines in transmittance measurement [Mizuno et al., 2016].

NMIJ is doing research on new terahertz detectors. We have demonstrated a terahertz pulse detection using a multilayer topological insulator [Makino et al., 2016].

We have developed a planar and a cylindrical scanner system for near-field antenna measurement using photonic sensor that is a few of grams in weight and a few of millimeters long. The systems are available about below 10 GHz.

We have developed an antenna radiation planar measurement system using photonic technologies. The systems are available about below 120 GHz.

We have developed a radio over fiber (RoF) transceiver usable attached to an RF network analyzer by microwave photonic technologies. It has a function of optical signal transmission and two-way conversion of E-O and O-E. Because the RoF transceiver is available being directly connected to antenna terminals and fed by only optical fibers, it does not affect the antenna characteristics and will become an ideal tool for antenna measurements [Kurokawa et al., 2016a] [Kurokawa et al., 2016b].

NMIJ is now researching and developing material characterization, i.e. dielectric permittivity measurements, at the microwave frequency. NMIJ has originally developed dielectric permittivity analysis with uncertainty optimization in the transmission/reflection measurement method for coaxial and waveguide lines [Kato Y., 2016a]. In the millimeter-wave frequency range, two types of free space measurement systems have been designed and installed. They are now being optimized and estimated the measurement uncertainty from 50 GHz to 330 GHz.

Furthermore, NMIJ as a pilot laboratory, switched from NIST, will start the Pilot study for dielectric permittivity measurement proposed by NIST as a former pilot laboratory in it. NMIJ is now considering and selecting the transfer material standards in the comparison. We are now proposing that two shapes of the transfer materials will be measured; plate samples by using the split-cylinder and/or split-post resonator methods, and block samples by using the waveguide method [Kato et al., 2016b] [Kato et al., 2016c].

A5. Power Attenuation and Impedance Measurements

The Applied Electronics Standards Group, the Radio-Frequency Group and the Electromagnetic Measurement Group in the elctrical standards area of NMIJ covers the A5 fields.

The NMIJ AC current ratio calibration system is renewed to extend the current range up to 100 amperes (current ratio up to 1000/1) in the frequency range between 45 Hz and 1 kHz [Yamada et al., 2015]. Over 1 kHz, the maximum input current is 50 amperes up to 4 kHz.

Temperature influence due to the increase of input current has been investigated and the uncertainty of the entire calibration system is updated. The detail will be prepared as a conference paper.

A new evaluation method for wideband voltage dividers has been proposed and presented at the CPEM 2016. The method is based on introduction of two phase-locked reference voltage generators to a voltage divider evaluation system for their input and reference output. The system constructed allows wide voltage ratio and wideband evaluation for voltage dividers up to 1 MHz. The wide voltage ratio also includes decimal ratios (such as 1.01 V/100 V).

JEMIC has provided the primary active/reactive power/energy standards for the power frequencies in the voltage range from 50 V to 120 V and in the current range from 2.5 A to 50 A [Kawagoe et al, 2010]. The standard individually measures voltage U and current I with two precise voltmeters and a shunt resistor, and phase θ with a precise digital phase meter. After these measurements, the active and reactive powers are calculated by $UI\cos\theta$ and $UI\sin\theta$, respectively. The representative expanded uncertainties under conditions of 100 V and 5 A are 22 μW/VA (power factor 1) and 10 μW/VA (power factor 0). In 2016, we calibrated 10 power meters and 70 energy meters.

JEMIC has been participating in APMP Key Comparison for "APMP.EM-K5.1" of AC power and energy.

The calibration system for WR-15 power meter was renewed. A frequency multiplier was substituted for a conventional backward-wave oscillator (BWO). NMIJ are developing a new calorimeter for a higher frequency range up to 330 GHz.

NMIJ has successfully established an RF attenuation standard system in the frequency range of 33 GHz to 50 GHz (Q-band), and started the jcss calibration service from June 2015 [Widarta et al., 2014]. The system is built by using the simple intermediate frequency (IF) receiver technique using a resistive step attenuators operated at 30 MHz, as an IF attenuation reference standard and a general-purpose receiver, as a level detector. By increasing the IF to 30 MHz, the noise effects caused by higher RF signals, such as the Q-band, can be kept small. This condition also allows us to use a general-purpose receiver as a sensitive level detector that facilitates the automation and long-term maintaining to the system. Traceability of the system then is ensured by performing periodic calibration to the IF attenuator reference standard at 30 MHz using the NMIJ attenuation standard system based on the voltage ratio of the IVD at 1 kHz.

Establishment of an attenuation reference primary standard in the frequency range of 110 GHz to 170 GHz has been also started [Widarta, 2016]. A millimeter wave VNA system, which consists of an intermediate frequency VNA and a set of millimeter wave S-parameter test extenders, is used as a measurement system. The traceability is ensured by the calibration to the intermediate frequency ports of the VNA using the calibrated step attenuator at 10.3 MHz.

NMIJ took an initiative to organize a CIPM Key Comparison of attenuation at 18 GHz, 26.5 GHz and 40 GHz using a step attenuator. This comparison has been registered in the KCDB under the identifier CCEM.RF-K26, with 15 laboratories (countries) declared to participate. Measurements of the first round loop can be said successful, although there were some delays in the delivery of the traveling standards between the participants. Currently, is in the second round loop and expected to be completed around June 2017.

A bilateral comparison of millimeter-wave attenuation in V band (50 GHz to 75 GHz) was performed between NMIJ and NMC [Iida et al., 2016a]. Good agreement of the measurement results between both laboratories was verified in the attenuation range up to 60 dB.

The terahertz waveguide flange, NMIJ developed, was standardized in the IEC 60154-2 standard. It provides precise connection and connection reproducibility [Horibe, 2016a] [Horibe ,2016b] [Horibe et al., 2016c] [Horibe et al., 2016d].

NMIJ is researching the material characterization at millimeter-wave frequency, precision on-wafer measurement techniques, printed electronics at millimeter-wave and non-linear load/source-pull measurement for GaN active devices [Horibe et al, 2016e] [Kishikawa et al., 2016a] [Kishikawa et al., 2016b] [Sakamaki et al., 2016a] [Sakamaki et al., 2016b]. Furthermore, electromagnetic sensing techniques are also researching for the agriculture products and food [Kon et al., 2016a] [Kon et al., 2016b].

Furthermore, NMIJ as a pilot laboratory is managing the CCEM key comparison (CCEM.RF-K5c.CL: S-parameter for PC3.5 in the range from 50 MHz to 33 GHz),, the APMP supplemental comparison (APMP.EM.RF-S5.CL: Dimensionally-derived characteristic impedance for PC7, PC2.4 and PC1.85) and will start the pilot study for material characterization.

NMIJ has demonstrated terahertz attenuator calibration using the calorimeter. We have shown measurement capability up to 12 dB with an expanded uncertainty of 0.19 - 0.84 dB (k = 2) at 1 THz [Iida et al., 2016b].

[References]

Akamatsu D., H. Inaba, K. Hosaka, M. Yasuda, A. Onae, T. Suzuyama, M. Amemiya, and F.-L. Hong [2014], “Spectroscopy and frequency measurement of the ^{87}Sr clock transition by laser linewidth transfer using an optical frequency comb,” Appl. Phys. Express, **7**, 012401 1-4Akamatsu D., M. Yasuda, H. Inaba, K. Hosaka, T. Tanabe, A. Onae and F.-L. Hong [2014a], “Frequency ratio measurement of ^{171}Yb and ^{87}Sr optical lattice clocks,” Optics Express, **22**, 7898-7905.

Akamatsu D., M. Yasuda, H. Inaba, K. Hosaka, T. Tanabe, A. Onae and F.-L. Hong [2014b], “Erratum: Frequency ratio measurement of ^{171}Yb and ^{87}Sr optical lattice clocks,” Optics Express, **22**, 32199.

Amagai Y., H. Fujiki, K. Shimizume, K. Kishino, and S. Hidaka [2015a], “Improvements in the Low-Frequency Characteristic and Sensitivity of a Thin-Film Multijunction Thermal Converter in Vacuum,” *IEEE Trans. Inst. Meas.* **64**(6), pp.1570 – 1575.

Amagai Y., A. Yamamoto, M. Akoshima, H. Fujiki, and N.-H. Kaneko [2015b], “AC/DC Transfer Technique for Measuring Thomson Coefficient: Toward Thermoelectric Metrology,” *IEEE Trans. Inst. Meas.* **64**(6), pp.1576 – 1581.

Bitou Y., T. Kobayashi and F.-L. Hong [2016], “Compact and inexpensive iodine-stabilized diode laser system with an output at 531 nm for gauge block interferometers,” Precision Engineering **47**, 528.

Chen S.-F., Y. Amagai and M. Maruyama and N.-H. Kaneko [2015], “Uncertainty Evaluation of a 10 V RMS Sampling Measurement System Using the AC Programmable Josephson Voltage Standard,” *IEEE Trans. Inst. Meas.* **64**(12), pp.3308 – 3314.

Domae A., N. Sakamoto, S. Kiryu and N.-H. Kaneko [2015b], “Development of 7.75 Ratio Voltage Divider Toward a Precise Measurement of Decade Resistance Based on the AC Quantized Hall Resistance,” *IEEE Trans. Inst. Meas*. **64** (6), pp. 1588 – 1594.

Domae A., T. Abe, M. Kumagai, M. Zama, T. Oe and N.-H. Kaneko [2015a], “Development and Evaluation of High-Stability Metal-Foil Resistor With a Resistance of 1 kΩ,” *IEEE Trans. Inst. Meas.* **64**(6) pp.1490 – 1495.

Fujieda M., T. Ido, H. Hachisu, T. Gotoh, H. Takiguchi, K. Hayasaka, K. Toyoda, K.Yonegaki, U. Tanaka, and S. Urabe [2016], "Frequency measurement system of optical clocks withtout a flywheel oscillator," IEEE TUFFC, **63**, 12, 2231-2236.

Fujisaki H., Y. Imai, K. Nishida, M. Mitaki, M. Kitano, and K. Sugiyama [2016], "Single-ion spectroscopy of the $^2S_{1/2}$ – $^2D_{5/2}$ transition in $^{138}Ba^+$ and laser cooling of odd-isotope Ba^+," European Conference on Trapped Ions 2016, poster No.20.

Hachisu H., M. Fujieda, S. Nagano, T. Gotoh, A. Nogami, T. Ido, St. Falke, N. Huntemann, C. Grebing, B. Lipphardt, Ch. Lisdat, and D. Piester [2014], "Direct comparison of optical lattice clocks with an intercontinental baseline of 9000 km," Opt. Lett. **39**, 4072-4075.

Hachisu H. and T. Ido [2015], "Intermittent optical frequency measurements to reduce the dead time uncertainty of frequency link," Jpn. J. Appl. Phys. **54**, 112401 1-7.

Horibe M. [2016a], "Connection Torque Consideration for Waveguide Flange at Millimeter-wave and Terahertz Frequencies," *ARFTG conference digests.*

Horibe M. [2016b], "Low Cost, High Performance of Coplanar Waveguide Fabricated by Screen Printing Technology," *IEICE TRANSACTIONS ON ELECTRONICS*, E99-C-10, pp.1094-1099.

Horibe M., Ryoko Kishikawa, Ryo Sakamaki, Yuto Kato, Seitaro Kon [2016c], "Improvement of Uncertainty Analysis for Waveguide VNA Measurement at Terahertz Frequency," *CPEM2016 Digest.*

Horibe M., Ryoko Kishikawa [2016d], "Primary Standard and Calibration of Scattering Parameter up to 12 GHz for Type N, 75 ohms connector," *CPEM2016 Digest.*

Horibe M., Ryo Sakamaki [2016e], "Performance Evaluations of Dielectric Waveguide for Millimeter-wave On-Wafer Measurements," *ARFTG Conference digest.*

Huang Y-J, M. Fujieda, and H. Takiguchi. [2016], "Stability improvement of an operational two-way satellite time and frequency transfer system," Metrologia, **53**, 881-890.

Ido T., H. Hachisu, F. Nakagawa and Y. Hanado [2016], "Rapid evaluation of time scale using an optical clock," J. Phys. Conf. Ser. **723**, 012041 1-6.

Iida H., T. Y. Wu [2016a], "NMC–NMIJ bilateral comparison of millimeter-wave attenuation in WR-15 waveguide band at 50 GHz and 54 GHz," *Measurement* **82**, 155-160.

Iida H., M. Kinoshita, K. Amemiya [2016b], "Calibration of a Terahertz Attenuator by a DC Power Substitution Method," *IEEE Trans. Instrum. Meas.*, DOI: 10.1109/TIM.2016.2637498, IEEE Early Access Article.

Ikegami T. et al. [2016]. "Autonomous cryogenic sapphire oscillators employing low vibration pulse-tube cryocoolers at NMIJ," J. Phys. Conference Series. **723**, 012032.

Imai Y., T. Nishi, M. Nishizaki, S. Kawajiri, Y. Muroki, R. Ikuta, K. Matsumoto, M. Kitano, and K. Sugiyama [2016], "Single-ion spectroscopy system for the $^2S_{1/2}(F=0)$ – $^2D_{3/2}(F=2)$ transition in $^{171}Yb^+$," Radio Science, **51**, 1385-1395.

Ito H., S. Nagano, M. Kumagai, M. Kajita, and Y. Hanado [2013] "Terahertz frequency counter with uncertainty at the 10-17 level," Appl. Phys. Exp. **6**, 102202 1-3.

Kajita M, G. Gopakumar, M. Abe, M. Hada, and M. Keller [2014] "Test of m_p/m_e changes using vibrational transitions in N_2^+," Phys. Rev. A **89**, 032509 1-6.

Kajita M. [2015] "N_2^+ quadrupole transitions with small Zeeman shift," Phys. Rev. A **92**, 043423 1-6.

Kaneko N.-H., T. Oe; T. Abe, M. Kumagai and M. Zama [2016a], "Development of 1 Ω and 10 Ω Metal-Foil Standard Resistors," *IEEE Trans. Inst. Meas.*, DOI: 10.1109/TIM.2016.2611318, IEEE Early Access Article.

Kaneko N.-H., S. Nakamura, Y. Okazaki [2016b], "A review of Quantum Current Standards," *Meas. Sci. Technol.* **27**, 032001(20).

Kato Y., Masahiro Horibe [2016a], "Permittivity measurement using a long fixture to eliminate reflection effect at fixture ends," *CPEM2016 Digest.*

Kato Y., Masahiro Horibe [2016b], "Permittivity measurements and associated uncertainties up to 110 GHz in circular-disk resonator method," *Proceedings of European Microwave Week 2016.*

Kato Y., Masahiro Horibe [2016c], "Permittivity measurements for high-permittivity materials at NMIJ using resonator methods," *CPEM2016 Digest.*

Kawagoe J. and T. Kawasaki [2010], "A New Precision Digital Phase Meter and Its Simple Calibration Method," *IEEE Trans. Instrum. Meas.*, **59**(2) pp. 396-403.

Kishikawa R., Masahiro Horibe, Shigeo Kawasaki (JAXA/ISAS) [2016a], "GaN Diode Measurement for Rectifier Design at 5.8 GHz," *Thailand-Japan Microwave.*

Kishikawa R., Shintaro Nakamura(JQA), Keiko Sato(JQA), Masahiro Horibe [2016b], "Metrological Connector Conversion Technique for Scattering Parameter Calibration," *CPEM2016 Digest.*

Kobayashi T., D. Akamatsu, K. Hosaka, H. Inaba, S. Okubo, T. Tanabe, M. Yasuda, A Onae, and F.-L. Hong [2015], "Compact iodine-stabilized laser operating at 531 nm with stability at the 10^{-12} level and using a coin-sized laser module," Optics Express **23**, 20749.

Kon S., Masahiro Horibe, Yuto Kato [2016a], "Frequency Optimization for Dynamic Measurements of Wide-range Moisture Content using Microwave," *Proceedings of TJMW2016*, pp.1-3.

Kon S., Masahiro Horibe, Yuto Kato [2016b], "Dynamic Measurements of Moisture Content using Microwave Signal and its Verification," *CPEM2016 Digest*, pp.119.

Kondo T. and K. Takefuji [2016], "An algorithm of wideband bandwidth synthesis for geodetic VLBI," Radio Science, **51**, DOI: 10.1002/2016RS006070.

Kurokawa S., M. Hirose [2016], "Measurement uncertainty of free space antenna factor for super broadband antenna using amplitude center modified equation," *CPEM2016 Digest.*

Kurokawa S., M. Hirose, Y. Toba, J. Ichijo [2016a], "Antenna measurement system using bi-directional optical fiber link system," *in Proc. 46th European Microwave Conference (EuMC)*, pp. 560 – 563.

Kurokawa S., M. Hirose, Y. Toba, M. Onizawa, J. Ichijo [2016b], “Antenna gain estimation for a single antenna measurement using bi-directional optical fiber link transceiver,” *in Proc. 2016 IEEE Conference on Antenna Measurements & Applications (CAMA)*, pp.1-4.

Makino K., S. Kuromiya, K. Takano, K. Kato, M. Nakajima, Y. Saito, J. Tominaga, H. Iida, M. Kinoshita, T. Nakano [2016], “THz Pulse Detection by Multilayered GeTe/Sb_2Te_3,” *ACS Appl. Mater. Interfaces* **8** (47) 32408-32413.

Maruyama M., H. Takahashi, K. Katayama, T. Yonezawa, T. Kanai, A. Iwasa, C. Urano, S. Kiryu and N.-H. Kaneko [2015a], “Evaluation of Linearity Characteristics in Digital Voltmeters Using a PJVS System With a 10-K Cooler,” *IEEE Trans. Inst. Meas.* **64**(6), pp.1613 – 1619.

Maruyama M., A. Iwasa, H. Yamamori, S.-F. Chen, C. Urano and N.-H. Kaneko [2015b], “Calibration System for Zener Voltage Standards Using a 10 V Programmable Josephson Voltage Standard at NMIJ,” *IEEE Trans. Inst. Meas.* **64**(6), pp.1606 – 1612.

Mitaki M., K. Sugiyama, and M. Kitano [2014], “Frequency stabilization of optical frequency comb using laser-diode pumped Kerr-lens mode-locked Yb:KYW laser for long-term continuous operation,” Advanced Solid State Lasers Conference, AM5a.27 1-3.

Mizuno M., H. Iida, M. Kinoshita, K. Fukunaga, Y. Shimada, C. Otani [2016], “Classification of terahertz spectrometer for transmittance measurements of refractive materials,” *IEICE Electron. Expr.* **13** (18) 20160532.

Nagano S., H. Ito, M. Kumagai, M. Kajita, and Y. Hanado [2013] “Microwave Synthesis From a Continuous Terahertz Oscillator Using Photocarrier Terahertz Frequency comb,” Opt. Lett. **30**, 2137-2139.

Nakamura S., Y. A. Pashkin, J.-S. Tsai and N.-H. Kaneko [2015], “Single-electron pumping by parallel SINIS turnstile for quantum current standard,” *IEEE Trans. Inst. Meas.* **64** (6) 1696-1701.

Nemitz N., T. Ohkubo, M. Takamoto, I. Ushijima, M. Das, N. Ohmae, and H. Katori [2016], “Frequency ratio of Yb and Sr clocks with 5x10-17 uncertainty at 150 seconds averaging time,” Nature Photonics **10**, 258-261.

Sakamaki R., Masahiro Horibe [2016a], "Development of Verification Process for On-Wafer Measurementat Millimeter-Wave Frequency," *CPEM2016 Digest.*

Sakamaki R., Masahiro Horibe [2016b], "Evaluation of Production Errors of Verification Devices with Precise Probing System," *URSI AP-RASC2016 Digest.*

Sekido M. et al., [2016], "An Overview of the Japanese GALA-V Wideband VLBI System," IVS 2016 General Meeting Proceedings "New Horizons with VGOS" Edited by Dirk Behrend.

Shimada Y., H. Iida, M. Kinoshita, "Recent Research Trends of Terahertz Measurement Standards [2015]," *IEEE Trans. Terahertz Sci. Tech.* **5** (6) 1166-1172Karen D. Baver, and Kyla L. Armstrong NASA/CP-2016-219016, 25-33.

Suemasa A., A. Shimo-oku, K. Nakagawa and M. Musha [2016], "Developments of highly frequency and intensity stabilized lasers for space gravitational wave detector DECIGO/B-DECIGO," Proc of ICSO2016, 2c-29.

Takahashi H., M. Maruyama, Y. Amagai, H. Yamamori, N.-H. Kaneko, S. Kiryu [2015], "Heat Transfer Analysis of a Programmable Josephson Voltage Standard Chip Operated with a Mechanical Cooler," *Physica C* **518**, pp.89 – 95.

Takamizawa A. et al. [2014], "Atomic fountain clock with very high frequency stability employing a pulse-tube-cryocooled sapphire oscillator," IEEE Transactions on Ultrasonics, Ferroelectrics, and Frequency Control, **61** (9), pp. 1463-1469.

Takamizawa A. et al. [2015a], "Preliminary evaluation of the cesium fountain primary frequency standard NMIJ-F2," IEEE Transactions on Instrumentation and Measurement, **64** (9), pp. 2504-2512.

Takamizawa A., S. Yanagimachi, T. Ikegami, R. Kawabata [2015b], "External cavity diode laser with frequency drift following natural variation in air pressure," Applied Optics, **54** (18), pp. 5777-5781.

Takamizawa A., S. Yanagimachi, T. Ikegami [2016], "External cavity diode laser with very-low frequency drift," Applied Physics Express **9**, 032704.

Takano T., M. Takamoto, I. Ushijima, N. Ohmae, T. Akatsuka, A. Yamaguchi, Y. Kuroishi, H. Munekane, B. Miyahara, and H. Katori [2016], "Geopotential measurements with synchronously linked optical lattice clocks," Nature Photonics **10**, 662-666.

Tanabe T., D. Akamatsu, T. Kobayashi, A. Takamizawa, S. Yanagimachi, T. Ikegami, T. Suzuyama, H. Inaba, S. Okubo, M. Yasuda, F.-L. Hong, A. Onae, and K. Hosaka [2015], "Improved frequency measurement of the $^{1}S_0$–$^{3}P_0$ clock transition in ^{87}Sr using a Cs fountain clock as a transfer oscillator," J. Phys. Soc. Jpn, **84**, 115002 1-2.

Tanabe T., D. Akamatsu, T. Kobayashi, A. Takamizawa, S. Yanagimachi, T. Ikegami, T. Suzuyama, H. Inaba, S. Okubo, M. Yasuda, F.-L. Hong, A. Onae, and K. Hosaka [2015], "Improved frequency measurement of the $^{1}S_0$–$^{3}P_0$ clock transition in ^{87}Sr using a Cs fountain clock as a transfer oscillator," J. Phys. Soc. Jpn, **84**, 115002 1-2.

Urano C., T. Yamada, M. Maezawa, K. Yamazawa, Y. Okazaki, Y. Fukuyama, N.-H. Kaneko, H. Yamamori, M. Maruyama; A. Domae, J. Tamba, S. Yoshida and S. Kiryu [2016], "Johnson Noise Thermometry Based on Integrated Quantum Voltage Noise Source," *IEEE Trans. Appl. Supercond.* **26**(3), pp.1800305(5).

Ushijima I., M. Takamoto, M. Das, T. Ohkubo, and H. Katori [2015], "Cryogenic optical lattice clocks," Nature Photonics **9**, 185-189.

Watanabe N., H. Tamura, N. Naka, M. Musha, and K. Nakagawa [2016], "Precision Spectroscopy of ^{87}Rb Rydberg states using an optical frequency synthesizer based on an optical frequency comb", The 25th International Conference on Atomic Physics (ICAP2016), Seoul, Korea, 24-29, Paper Mon-049.

Widarta A., Y. Kato [2014], "Establishment of RF Attenuation Standard in the Frequency Range of 30 GHz to 50 GHz at NMIJ," *CPEM2014 Digest*.

Widarta A. [2016], "Establishment of Attenuation Standards in the Frequency Range of 110 GHz to 170 GHz using a Millimeter Wave VNA System," *CPEM2016 Digest*.

Yamada T., and S. Kon [2015], "Error and Uncertainty Estimations for A Passive-CC-Based AC Current Ratio Standard at High Audio Frequencies," *IEEE Trans. Instr. Meas.*, **64**(6), pp.1546-1552.

Yamanaka K., N. Ohmae, I. Ushijima, M. Takamoto, and H. Katori [2015], “Frequency Ratio of ^{199}Hg and ^{87}Sr Optical Lattice Clocks beyond the SI Limit,” Physics Review Letters **114**, 230801.

Yano Y., W. Gao, S. Goka, and M. Kajita [2014], “Theoretical and experimental investigation of the light shift in Ramsey coherent population trapping,” Phys. Rev. A**90**, 013826 1-6.

Yano Y., S. Goka and M. Kajita [2015], “Two-step pulse observation for Raman-Ramsey coherent population trapping atomic clocks,” Appl. Phys. Exp. **8**, 012801 1-4.